Inorg. Chem. **2004**, *43*, 5422–5431

Immobilization of Oxomolybdenum Species in a Layered Double Hydroxide Pillared by 2,2′-Bipyridine-5,5′-dicarboxylate Anions

Sandra Gago, Martyn Pillinger,* Anabela A. Valente, Teresa M. Santos, João Rocha, and Isabel S. Gonçalves*

Department of Chemistry, CICECO, University of Aveiro, 3810-193 Aveiro, Portugal

Received February 25, 2004

A Zn,Al layered double hydroxide (LDH) with Zn/Al = 1.45 and containing nitrate anions was prepared by coprecipitation and characterized by powder X-ray diffraction, Zn K-edge extended X-ray absorption fine structure spectroscopy (EXAFS), thermogravimetric analysis, FTIR and FT Raman spectroscopy, and ^{27}Al MAS NMR spectroscopy. Three Zn···O and four Zn···M (M = Zn, Al) shells could be fitted to the low-temperature (40 K) EXAFS spectrum, in accordance with a model for an ordered cationic sheet. The nitrate anions were easily exchanged by 2,2′-bipyridine-5,5′-dicarboxylate anions, resulting in an increase in the basal spacing from 9 to 18 Å. The basal spacing of the pillared derivative indicates that the anions are arranged with their longest dimension nearly perpendicular to the host layers. This material exhibits a high encapsulating ability, as evidenced by its interaction with a dichloromethane solution of the dioxomolybdenum(VI) complex $MoO_2Cl_2(THF)_2$. A material with a metal loading of 11.2 wt % was obtained. Molybdenum K-edge EXAFS analysis could not substantiate the formation of a supported complex of the type $MoO_2Cl_2(N–N)$ but instead indicated the formation of unidentate-bridged entities of the type $[O_2Mo–O–MoO_2]$ with a metal–metal separation of 3.29 Å. The molybdenum-containing LDH was active as a catalyst for the liquid-phase epoxidation of *cis*-cyclooctene, 1-octene, and *trans*-2-octene using *tert*-butyl hydroperoxide as the oxygen source, yielding the corresponding epoxides as the only products. For reactions carried out with no additional solvent (other than *n*-decane) or in the presence of 1,2-dichloroethane, the solid catalyst could be recycled with no major loss of activity. Other tests confirmed that the systems functioned as true heterogeneous catalysts.

Introduction

Molybdenum(VI) complexes are versatile catalysts for the oxidation of organic compounds.[1] The most significant reaction in industry is the epoxidation of propylene to propylene oxide by alkyl hydroperoxides, catalyzed with high activity and selectivity by soluble Mo^{VI} compounds.[2] In recent years, complexes of the type $MoO(O_2)_2(L_1)(L_2)$ and $MoO_2X_2(L_1)(L_2)$ (X = Cl, Br, CH_3), with different combinations of base ligands L_1 and L_2, have been extensively investigated as catalysts for epoxidation reactions, usually employing *tert*-butyl hydroperoxide (TBHP) as the monooxygen source.[3,4] Important properties, such as the solubility of the complex and the Lewis acidity of the metal center, can be fine-tuned by variation of either X or L. These adjustments allow highly active and selective catalysts to be prepared.

Despite the good results obtained for oxomolybdenum(VI) complexes in homogeneous catalysis, increasing attention is being drawn to studying and developing heterogeneous catalysts since these can be easily separated from a reaction mixture and recycled, which is of significant industrial interest.[5] One approach is to link metal complexes to organic polymers and inorganic oxides by way of Lewis base ligands. For example, molybdenum(VI) complexes have been sup-

* Authors to whom correspondence should be addresed. E-mail: igoncalves@dq.ua.pt (I.S.G.), mpillingcr@dq.ua.pt (M.P.). Tel.: 00351-234-370200 (I.S.G.), 00351-234-378123 (M.P.). Fax: 00351-234-370084 (I.S.G.).

(1) Jörgensen, K. A. *Chem. Rev.* **1989**, *89*, 431. Dickman, M. H.; Pope, M. T. *Chem. Rev.* **1994**, *94*, 569.

(2) Brégeault, J.-M. *J. Chem. Soc., Dalton Trans.* **2003**, 3289. Parshall, G. W.; Ittel, S. D. *Homogeneous Catalysis: The Applications and Chemistry of Catalysis by Soluble Transition Metal Complexes*; Wiley: New York, 1992.

(3) Thiel, W. R.; Angstl, M.; Priermeier, T. *Chem. Ber.* **1994**, *127*, 2373. Thiel, W. R.; Angstl, M.; Hansen, N. *J. Mol. Catal. A: Chem.* **1995**, *103*, 5. Thiel, W. R.; Priermeier, T. *Angew. Chem., Int. Ed. Engl.* **1995**, *34*, 1737. Thiel, W. R.; Eppinger, J. *Chem.—Eur. J.* **1997**, *3*, 696.

(4) (a) Kühn, F. E.; Herdtweck, E.; Haider, J. J.; Herrmann, W. A.; Gonçalves, I. S.; Lopes, A. D.; Romão, C. C. *J. Organomet. Chem.* **1999**, *583*, 3. (b) Kühn, F. E.; Lopes, A. D.; Santos, A. M.; Herdtweck, E.; Haider, J. J.; Romão, C. C.; Santos, A. G. *J. Mol. Catal. A: Chem.* **2000**, *151*, 147. (c) Kühn, F. E.; Santos, A. M.; Lopes, A. D.; Gonçalves, I. S.; Herdtweck, E.; Romão, C. C. *J. Mol. Catal. A: Chem.* **2000**, *164*, 25.

10.1021/ic049755n CCC: $27.50
Published on Web 07/21/2004

ported on imidazole-containing polymers and shown to be recyclable catalysts for olefin epoxidation with TBHP.[6] With inorganic supports, a general strategy is to use functional alkoxy silanes.[7] Thiel and co-workers prepared covalently anchored complexes of the type $MoO(O_2)_2(L-L)$ using the mesoporous silica MCM-41 derivatized with a bidentate pyrazolylpyridine ligand.[8] Molybdenum(VI) complexes of the type $MoO_2Cl_2(L_1)(L_2)$ have also been immobilized in MCM-41 derivatized with monodentate nitrile and bidentate N,N-ligands.[9]

Another method for the immobilization of oxomolybdenum complexes was reported by Corma and co-workers, involving the insertion of the anion $[MoO_2(O_2CC(S)Ph_2)_2]^{2-}$ into the interlamellar space of a Zn,Al layered double hydroxide (LDH).[10] The immobilized complex functioned as an effective heterogeneous catalyst for the oxidation of thiols by either dioxygen or air. LDHs, also known as anionic clays or hydrotalcite-like (HT-like) compounds, have the general composition $[M^{2+}_{1-x}M^{3+}_x(OH)_2](A^{n-})_{x/n}\cdot zH_2O$ (M^{2+} = Ca^{2+}, Mg^{2+}, Zn^{2+}, Ni^{2+}, etc.; M^{3+} = Al^{3+}, Cr^{3+}, Ga^{3+}, etc.) and a structure involving positively charged mixed metal hydroxide layers separated by charge-balancing anions and water molecules.[11] The gallery anions A^{n-} are exchangeable, giving rise to a rich intercalation chemistry.[12] Many different types of metal coordination compounds and oxometalates have been intercalated into LDHs by ion exchange, including phthalocyanines, cyanocomplexes, oxalate complexes, and polyoxometalates.[11-13]

LDHs containing metal complexes of chelating ligands, namely NTA (nitrilotriacetate) and EDTA (ethylenediaminetetraacetate), have also been prepared, either directly by intercalation of the metal complex or indirectly by forming the metal complex between the host layers following intercalation of the ligand.[14,15] LDHs containing chelating ligands can be viewed as solid-state complexation materials for metal ions. Possible applications include the recovery of transition and/or radioactive metals from aqueous solution and the heterogenization of homogeneous catalysts. In this work, a Zn,Al LDH pillared by 2,2′-bipyridine-5,5′-dicarboxylate (BDC) anions has been prepared and examined as a support for oxomolybdenum complexes. Catalytic tests have been carried out for the epoxidation of olefins by TBHP.

Experimental Section

Reagents. The starting materials $Zn(NO_3)_2\cdot 6H_2O$, $Al(NO_3)_3\cdot 9H_2O$, 50% aqueous NaOH, $NaNO_3$, 2,2′-bipyridine-5,5′-dicarboxylic acid, KOH, and MoO_2Cl_2 were obtained from commercial sources and used as received. Organic solvents were dried by refluxing over appropriate drying agents, distilled under nitrogen, and stored over 4 Å molecular sieves. The complexes $MoO_2Cl_2(THF)_2$ (**1**) and MoO_2Cl_2(4,4′-dimethyl-2,2′-bipyridine) (**2**) were prepared using published procedures.[4]

Characterization Methods. Microanalyses for CHN were carried out at the Instituto de Tecnologia Química e Biológica, Oeiras, Portugal (C. Almeida). Zn, Al, and Mo were determined by ICP-OES at the Central Laboratory for Analysis, University of Aveiro (E. Soares). Powder X-ray diffraction (XRD) data were collected at room temperature on a Philips X'pert diffractometer with a curved graphite monochromator (Cu Kα radiation), in a Bragg−Brentano para-focusing optics configuration. Samples were step-scanned in 0.02° 2θ steps with a counting time of 1 s/step. Thermogravimetric analysis (TGA) was performed using a Shimadzu TGA-50 system at a heating rate of 5 °C min^{-1} under air. Nitrogen adsorption measurements at 77 K were recorded gravimetrically using a CI electronic MK2-M5 microbalance and an Edwards Barocel pressure sensor. Prior to measurement, the solids were outgassed at 298 K overnight to give a residual pressure of ca. 10^{-4} mbar.

IR spectra were obtained with KBr pellets using a FTIR Mattson-7000 infrared spectrophotometer. Raman spectra were recorded on a Brüker RFS100/S FT instrument (Nd:YAG laser, 1064 nm excitation, InGaAs detector). Solid-state NMR spectra were measured at 100.62 MHz for ^{13}C and 104.26 MHz for ^{27}Al with a (9.4 T) wide-bore Bruker Avance 400 spectrometer. ^{13}C CP MAS NMR spectra were acquired with a 3.5 μs 90° proton pulse and 2 ms contact time with spinning rates 7−8.5 kHz and 4 s recycle delays. Chemical shifts are quoted in ppm from TMS. Single-quantum ("conventional") ^{27}Al MAS NMR spectra were acquired using short and powerful radio frequency pulses (0.6 μs, corresponding to $\pi/12$ pulses), a spinning rate of 14 kHz, and a recycle delay of 1 s. Chemical shifts are quoted in ppm from $Al(H_2O)_6^{3+}$.

X-ray absorption spectra were measured in transmission mode on beamline BM29 at the ESRF (Grenoble, France),[16] operating at 6 GeV in hybrid mode with typical currents of 170−190 mA. The Mo K-edge spectra were recorded at room temperature, and the Zn K-edge spectra, at ca. 40 K (using an Oxford Instruments cryostat filled with He exchange gas). Scans were set up to record the preedge at 5 eV steps and the postedge region in 0.025−0.05 $Å^{-1}$ steps, giving a total acquisition time of ca. 45 min/scan. The order-sorting double Si(111) crystal monochromator was detuned by 50% to ensure harmonic rejection. Solid samples were diluted with BN and pressed into 13 mm pellets. Ionization chamber

(5) Sheldon, R. A.; Arends, I. W. C. E.; Lempers, H. E. B. *Catal. Today* **1998**, *41*, 387. Sheldon, R. A.; Wallau, M.; Arends, I. W. C. E.; Schuchardt, U. *Acc. Chem. Res.* **1998**, *31*, 485. Sherrington, D. C. *Catal. Today* **2000**, *57*, 87.

(6) (a) Leinonen, S.; Sherrington, D. C.; Sneddon, A.; McLoughlin, D.; Corker, J.; Canevali, C.; Morazzoni, F.; Reedijk, J.; Spratt, S. B. D. *J. Catal.* **1999**, *183*, 251. (b) Miller, M. M.; Sherrington, D. C. *J. Catal.* **1995**, *152*, 368. (c) Miller, M. M.; Sherrington, D. C. *J. Catal.* **1995**, *152*, 377.

(7) Moller, K.; Bein, T. *Chem. Mater.* **1998**, *10*, 2950. De Vos, D. E.; Dams, M.; Sels, B. F.; Jacobs, P. A. *Chem. Rev.* **2002**, *102*, 3615.

(8) Jia, M.; Thiel, W. R. *Chem. Commun.* **2002**, 2392. Jia, M.; Seifert, A.; Thiel, W. R. *Chem. Mater.* **2003**, *15*, 2174.

(9) (a) Ferreira, P.; Gonçalves, I. S.; Kühn, F. E.; Lopes, A. D.; Martins, M. A.; Pillinger, M.; Pina, A.; Rocha, J.; Romão, C. C.; Santos, A. M.; Santos, T. M.; Valente, A. A. *Eur. J. Inorg. Chem.* **2000**, 2263. (b) Nunes, C. D.; Valente, A. A.; Pillinger, M.; Fernandes, A. C.; Romão, C. C.; Rocha, J.; Gonçalves, I. S. *J. Mater. Chem.* **2002**, *12*, 1735. (c) Nunes, C. D.; Pillinger, M.; Valente, A. A.; Rocha, J.; Lopes, A. D.; Gonçalves, I. S. *Eur. J. Inorg. Chem.* **2003**, 3870.

(10) Cervilla, A.; Corma, A.; Fornés, V.; Llopis, E.; Palanca, P.; Rey, F.; Ribera, A. *J. Am. Chem. Soc.* **1994**, *116*, 1595. Cervilla, A.; Llopis, E.; Ribera, A.; Corma, A.; Fornés, V.; Rey, F. *J. Chem. Soc., Dalton Trans.* **1994**, 2953. Corma, A.; Rey, F.; Thomas, J. M.; Sankar, G.; Greaves, G. N.; Cervilla, A.; Llopis, E.; Ribera, A. *J. Chem. Soc., Chem. Commun.* **1996**, 1613.

(11) *Layered Double Hydroxides: Present and Future*; Rives, V., Ed.; Nova Science Publishers: New York, 2001.

(12) Khan, A. I.; O'Hare, D. *J. Mater. Chem.* **2002**, *12*, 3191.

(13) Rives, V.; Ulibarri, M. A. *Coord. Chem. Rev.* **1999**, *181*, 61.

(14) Tarasov, K. A.; O'Hare, D.; Isupov, V. P. *Inorg. Chem.* **2003**, *42*, 1919. Tsyganok, A. I.; Suzuki, K.; Hamakawa, S.; Takehira, K.; Hayakawa, T. *Chem. Lett.* **2001**, 24. Tarasov, K. A.; Isupov, V. P.; Chupakhina, L. E. *Russ. J. Inorg. Chem.* **2000**, *45*, 1659.

(15) Gutmann, N. H.; Spiccia, L.; Turney, T. W. *J. Mater. Chem.* **2000**, *10*, 1219. Kaneyoshi, M.; Jones, W. *Mol. Cryst. Liq. Cryst.* **2001**, *356*, 459. Kaneyoshi, M.; Jones, W. *J. Mater. Chem.* **1999**, *9*, 805.

(16) Filipponi, A.; Borowski, M.; Bowron, D. T.; Ansell, S.; Cicco, A. D.; Panfilis, S. D.; Itiè, J.-P. *Rev. Sci. Instrum.* **2000**, *71*, 2422.

detectors were filled with Ar to give 30% absorbing I_o (incidence) and 70% absorbing I_t (transmission). The programs EXCALIB and EXBACK (SRS Daresbury Laboratory, Warrington, U.K.) were used in the usual manner for calibration and background subtraction of the raw data. EXAFS curve-fitting analyses, by least-squares refinement of the non-Fourier-filtered k^3-weighted EXAFS data, were carried out using the program EXCURVE (version EXCURV98[17]) using fast curved wave theory.[18] Phase shifts were obtained within this program using ab initio calculations based on the Hedin Lundqvist/von Barth scheme. Unless otherwise stated, the calculations were performed with single scattering contributions only. For each EXAFS simulation the validity of extra parameters was checked using a comparative reduced χ^2 method.[19]

Synthesis of Zn,Al−NO$_3$.[20] A solution of $Zn(NO_3)_2 \cdot 6H_2O$ (6.84 g, 23 mmol) and $Al(NO_3)_3 \cdot 9H_2O$ (4.50 g, 12 mmol) in decarbonated deionized (DD) water (60 mL) was added dropwise under nitrogen to a solution of 50% NaOH (5.6 g, 70 mmol) and $NaNO_3$ (3.4 g, 40 mmol) in DD water (60 mL) with good mixing. The resulting gellike slurry was aged at 85 °C for 18 h and then cooled to ambient temperature, filtered and washed several times with DD water, and stored as an aqueous slurry in a closed container (total volume ca. 100 mL). For analysis, 20 mL of this slurry was filtered and the solid dried at room temperature under reduced pressure in a vacuum desiccator. Anal. Calcd for $Zn_{2.9}Al_2(OH)_{9.8}(NO_3)_2 \cdot 3.5H_2O$: Zn, 31.75; Al, 9.03; N, 4.69; H, 2.83. Found: Zn, 31.80; Al, 9.20; N, 4.56; H, 2.72. TGA up to 150 °C revealed a sample weight loss of 7.3% (calcd for loss of 3.5 H_2O: 10.5%). IR (KBr, cm^{-1}): 3529 (sh), 3433 (vs), 2739 (sh), 2426 (w), 2395 (m), 1762 (s), 1622 (br), 1436 (sh), 1383 (vs), 1021 (w), 971 (sh), 891 (sh), 826 (m), 703 (br), 620 (m), 552 (w), 425 (vs), 314 (s). Raman (cm^{-1}): 3427, 1641, 1390, 1055, 717, 551, 488, 257, 196, 100, 85. ^{27}Al MAS NMR: $\delta = 15.7$.

Synthesis of Zn,Al−BDC. A total of 2 equiv of KOH in DD water (20 mL) was added to a solution/suspension of 2,2′-bipyridine-5,5′-dicarboxylic acid (0.53 g, 2.16 mmol) (ca. 30% in excess over that theoretically required for complete exchange of nitrate anions) in DMF (25 mL) at 70 °C. An aqueous suspension of Zn,Al−NO_3 (33 mL, 1.0 g LDH) was then added and the mixture stirred for 48 h at 50 °C. The solid product was isolated by filtration, washed several times with decarbonated water, and dried at room temperature under reduced pressure in a vacuum desiccator. Anal. Calcd for $Zn_{2.9}Al_2(OH)_{9.8}[bipy(COO)_2] \cdot 7H_2O$: Zn, 24.36; Al, 6.93; C, 18.51; N, 3.60; H, 3.86. Found: Zn, 23.90; Al, 6.88; C, 18.42; N, 3.66; H, 3.60. TGA up to 150 °C revealed a sample weight loss of 14.1% (calcd for loss of 7 H_2O: 16.2%). IR (KBr, cm^{-1}): 3396 (br), 1613 (vs), 1594 (sh), 1559 (w), 1540 (sh), 1471 (w), 1390 (vs), 1305 (sh), 1259 (sh), 1247 (w), 1160 (w), 1136 (w), 1037 (m), 952 (sh), 840 (m), 775 (m), 726 (sh), 620 (m), 564 (w), 426 (vs), 399 (w), 326 (w). Raman (cm^{-1}): 3400, 3188, 3081, 1596, 1494, 1406, 1386, 1366, 1316, 1287, 1263, 1239, 1145, 1041, 860, 809, 671, 649, 553, 412, 310, 107, 85. ^{13}C CP MAS NMR: $\delta =$ 120.7, 131.5, 134.5, 140.9, 149.1 (all bipy-C), 169.3 (C-CO_2^-). ^{27}Al MAS NMR: $\delta = 15.1$.

Synthesis of Zn,Al−BDC/Mo. The adduct $MoO_2Cl_2(THF)_2$ was prepared by evaporating to dryness a solution of MoO_2Cl_2 (0.223 g, 1.12 mmol) in THF (10 mL). CH_2Cl_2 (10 mL) was added and the resulting colorless solution added dropwise to a suspension of Zn,Al−BDC (0.75 g, 0.96 mmol bipy) in CH_2Cl_2 (10 mL). The reaction mixture was stirred for 1 h at room temperature. Following this, the pale blue solid was filtered out, washed several times with CH_2Cl_2, and dried in vacuo. Anal. Found: Mo, 11.2. TGA up to 150 °C revealed a sample weight loss of 11.8%. IR (KBr, cm^{-1}): 3430 (br), 1617 (s), 1596 (sh), 1559 (m), 1472 (w), 1381 (s), 1303 (w), 1260 (m), 1223 (sh), 1163 (m), 1137 (m), 1038 (s), 949 (sh), 935 (sh), 898 (sh), 869 (sh), 842 (w), 806 (sh), 777 (m), 710 (w), 669 (sh), 621 (w), 562 (sh) 426 (s), 324 (w). Raman (cm^{-1}): 3387, 1596, 1493, 1313, 1285, 1256, 1145, 978. ^{13}C CP MAS NMR: $\delta =$ 24.7 (THF), 67.1 (THF), 122.0, 134.5, 141.2, 148.6 (all bipy-C), 168.0 (C-CO_2^-). ^{27}Al MAS NMR: $\delta = 15.1$.

Catalysis Experiments. The epoxidation of different olefins was carried out at 55 °C under air in a batch reactor equipped with a magnetic stirrer. The reactor was loaded with supported catalyst (175 mg) or complex **2** (73 μmol), 7.3 mmol of olefin (1% molar ratio of catalyst/substrate), and 11 mmol of TBHP (5.5 M in decane). Samples were withdrawn periodically and analyzed using a gas chromatograph (Varian 3800) equipped with a capillary column (SPB-5, 20 m × 0.25 mm × 0.25 μm) and a flame ionization detector.

Results and Discussion

Synthesis of Zn,Al−NO$_3$ and Zn,Al−BDC Intercalates. A Zn,Al LDH containing nitrate anions was prepared as described previously using a coprecipitation method.[20] Elemental analysis indicated the composition $Zn_{2.9}Al_2(OH)_{9.8}(NO_3)_2 \cdot 3.5H_2O$ [$x = Al^{3+}/(Zn^{2+} + Al^{3+}) = 0.41$]. The final Zn/Al ratio of 1.45 is lower than that in the starting solution (2.0), indicating an incomplete precipitation of the divalent anion. This may be due to the fact that the pH of the reaction mixture after hydrothermal treatment (7−8) was on the low end of the range usually considered appropriate for the synthesis of Zn,Al LDHs (7−9).[11] In naturally occurring hydrotalcite-type minerals, the value of x falls in the range 0.22−0.33. The value of 0.33 has been assumed to be the upper limit of x, even in synthetic LDHs, on the basis of crystal chemical considerations.[21] However, in the Zn,Al system, carbonate-containing materials have been prepared and characterized with $x = 0.3-0.4$.[22]

The powder XRD pattern obtained for Zn,Al−NO_3 is typical of reasonably well-crystallized HT-like materials, exhibiting sharp and symmetric 00l reflections (Figure 1). The peaks have been indexed in rhombohedral symmetry, although the presence of broad and asymmetric 01l reflections indicates disorder in the layer stacking, such as a turbostratic structure or an intergrowth of the rhombohedral and hexagonal polytypes.[23] No evidence was found for the presence of $Al(OH)_3$ (gibbsite at 18.4° or bayerite at 18.8°). The lattice parameter a was calculated as $2d_{110} = 3.06$ Å. In their study of Al-rich Zn,Al HT-like compounds, Thevenot et al. reported that the lattice parameter a decreased continuously as a function of x.[22] Using their data, an LDH with $x = 0.41$ is expected to have a lattice parameter $a = 3.056$ Å,

(17) Binsted, N. EXCURV98, CCLRC Daresbury Laboratory computer program, 1998.
(18) Gurman, S. J.; Binsted, N.; Ross, I. *J. Phys. C* **1984**, *17*, 143. Gurman, S. J.; Binsted, N.; Ross, I. *J. Phys. C* **1986**, *19*, 1845.
(19) O'Donnell, K. P.; Mosselmans, J. F. W.; Martin, R. W.; Pereira, S.; White, M. E. *J. Phys.: Condens. Matter* **2001**, *13*, 6977.
(20) Evans, J.; Pillinger, M.; Zhang, J. *J. Chem. Soc., Dalton Trans.* **1996**, 2963.
(21) Brindley, G. W.; Kikkawa, S. *Am. Mineral.* **1979**, *64*, 836.
(22) Thevenot, F.; Szymanski, R.; Chaumette, P. *Clays Clay Miner.* **1989**, *37*, 396.
(23) Bellotto, M.; Rebours, B.; Clause, O.; Lynch, J.; Bazin, D.; Elkaïm, E. *J. Phys. Chem.* **1996**, *100*, 8527.

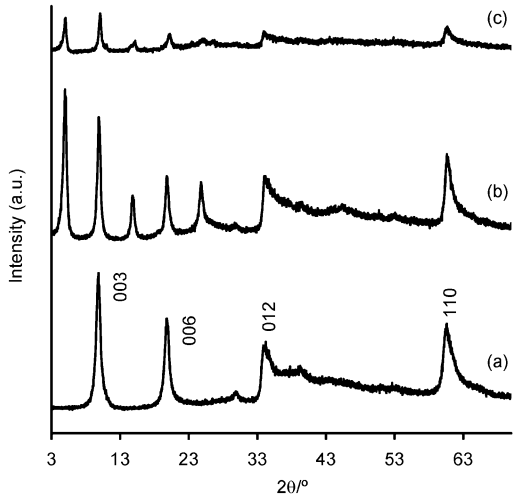

Figure 1. Powder XRD patterns of the intercalates: (a) Zn,Al−NO_3, (b) Zn,Al−BDC, and (c) Zn,Al−BDC/Mo.

in good agreement with the results obtained in this work for the Zn,Al−NO_3 LDH.

The area/unit charge in the brucite-like layer for Zn,Al−NO_3 is given by $A_c = (a^2 \sin 60)/x = 19.8$ Å^2. Xu and Zeng prepared a series of Mg,Al−NO_3 LDHs with different Mg/Al ratios.[24] The area occupied by a nitrate anion in a "flat-lying" model was estimated to be 23.1 Å^2 (a square with side lengths of 4.95 and 4.66 Å). It follows that the charge-balancing anions in Zn,Al−NO_3 cannot be arranged in a monolayer with the molecular planes parallel to the host layers. One solution is to have the NO_3^- anions tilted with a slant angle in the gallery space.[24] Given that the thickness of a brucite-like layer is 4.77 Å, the basal spacing for NO_3^- anions in a vertical orientation would be at least 9.43 Å (=4.77 Å + 4.66 Å). For our material the basal spacing is 8.98 Å (=d_{003}), and therefore, the nitrate anions would have to be tilted at an angle of less than 90° to the host layers. In this orientation the symmetry of the NO_3^- anions would be C_{2v} (instead of D_{3h} for the "flat-lying" model).

The vibrational spectra provide further clues about the anion configuration in Zn,Al−NO_3. In the IR spectrum, two bands at 826 and 1383 cm^{-1} are attributed to the out-of-plane symmetric deformation mode ν_2 and the antisymmetric stretching mode ν_3, respectively.[25] The antisymmetric deformation mode ν_4 is observed at 668 cm^{-1}, although it is largely obscured by the host lattice modes. The Raman spectrum contains a very strong band at 1055 cm^{-1} assigned to the symmetric stretching mode ν_1 and also a weak band at 717 cm^{-1} for the ν_4. If the symmetry of the nitrate anions in Zn,Al−NO_3 was D_{3h}, the ν_1 mode would not be IR active. However, a weak band was observed at 1021 cm^{-1}, suggesting that the symmetry has been lowered, perhaps to C_{2v}. The "tilt-lying" model therefore seems plausible.

An alternative model for the anion arrangement in Zn,Al−NO_3 must also be considered, in which the nitrate anions alternatively stick to the top and bottom planes of the same gallery while at the same time maintaining a horizontal orientation with respect to the brucite-like layers (so-called "stick-lying" model[24]). A lowering of symmetry from D_{3h} might be caused by a strong interaction with the hydroxyl layers. Support for this model comes from the appearance of the IR band associated with ν_{OH} stretching. For Zn,Al−NO_3 the band is separated into two components at 3529 and 3433 cm^{-1}, very similar to that reported by Xu and Zeng for a Mg,Al−NO_3 LDH with $x = 0.33$.[24] These authors took this as evidence for the "stick-lying" model, where one group of layer hydroxyls interacts directly with NO_3^- (giving rise to the lower wavenumber component) and one does not (giving rise to the higher wavenumber component).

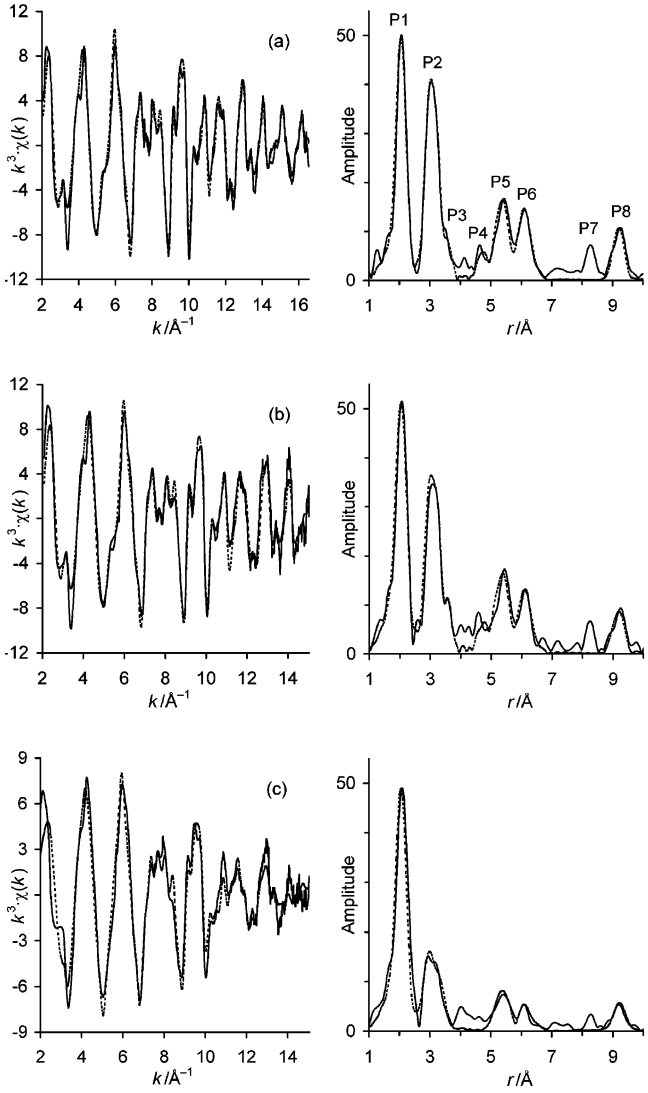

Figure 2. Low-temperature (40 K) Zn K-edge EXAFS and Fourier transforms of (a) Zn,Al−NO_3, (b) Zn,Al−BDC, and (c) Zn,Al−BDC/Mo. The solid lines represent the experimental data, and the dashed lines show the best fits using the parameters given in Table 1.

Figure 2 shows the Zn K-edge k^3-weighted EXAFS spectrum and Fourier transform (FT) of Zn,Al−NO_3. Good quality EXAFS data were obtained up to 16.5 Å^{-1}, and several peaks can be observed in the FT up to 9 Å. Peaks P1, P3, and P4 correspond to the first three oxygen shells, while P2 and P5−P8 are mainly caused by the metallic neighbors at a, $\sqrt{3}a$, $2a$, $\sqrt{7}a$, and $3a$ (where a is the cation−

(24) Xu, Z. P.; Zeng, H. C. *J. Phys. Chem. B* **2001**, *105*, 1743.
(25) Kloprogge, J. T.; Wharton, D.; Hickey, L.; Frost, R. L. *Am. Mineral.* **2002**, *87*, 623.

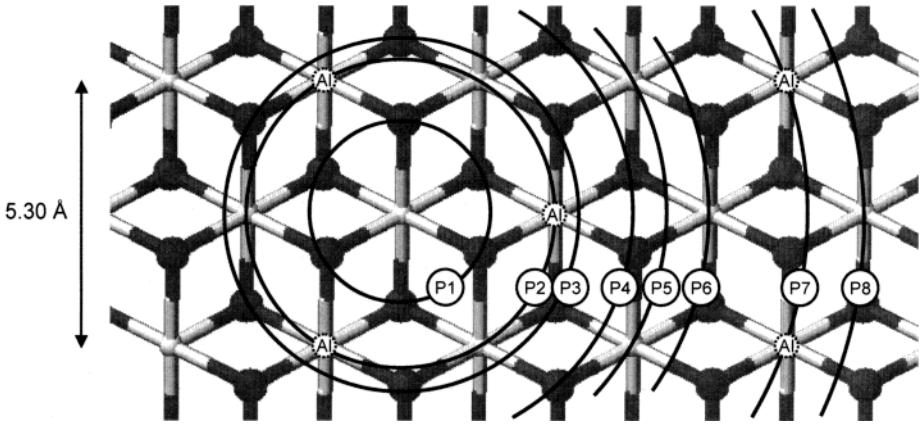

Figure 3. Model of an ordered cationic sheet for a Zn,Al LDH with Zn/Al = 2. The circles or portion circle define the backscattering shells for Zn centers, which contribute to the EXAFS signal.

Table 1. Zn K-Edge and Mo K-Edge EXAFS-Derived Structural Parameters for Zn,Al−NO_3, Zn,Al−BDC, Zn,Al−BDC/Mo, and MoO_2Cl_2(4,4′-dimethyl-2,2′-bipyridine) (**2**)

compd	edge	atom	CN[a]	r (Å)	$2\sigma^2$ (Å^2)[b]	E_f (eV)[c]	R (%)[d]
Zn,Al−NO_3[e]	Zn K	O	5.5(2)	2.075(2)	0.0118(5)	−3.3(2)	21.7
		ZA1[f]	6.0(6)	3.059(2)	0.0072(3)		
		O	6.0(10)	3.543(10)	0.0172(27)		
		O	12.0(60)	4.776(19)	0.0270(57)		
		Zn	6.0(15)	5.299(5)	0.0121(9)		
		ZA2[f]	6.0	6.139(5)	0.0079(9)		
		Al	6.0	9.192(7)	0.0069(11)		
Zn,Al−BDC[e]	Zn K	O	6.0(3)	2.070(3)	0.0143(7)	−3.0(3)	25.2
		ZA1[g]	6.0(7)	3.058(2)	0.0080(4)		
		O	6.0(10)	3.551(11)	0.0153(29)		
		O	12.0(60)	4.773(25)	0.0295(79)		
		Zn	6.0(15)	5.291(6)	0.0117(10)		
		ZA2[g]	6.0	6.127(7)	0.0085(12)		
		Al	6.0	9.169(11)	0.0086(19)		
Zn,Al−BDC/Mo[e]	Zn K	O	5.0(2)	2.077(4)	0.0117(7)	−5.6(4)	34.0
		ZA1[h]	6.0	3.075(6)	0.0174(12)		
		Zn	6.0	5.304(12)	0.0197(25)		
		ZA2[h]	6.0	6.149(20)	0.0191(40)		
		Al	6.0	9.210(19)	0.0132(35)		
2[i]	Mo K	O	2.0(1)	1.705(1)	0.0026(2)	−9.2(5)	25.2
		N	2.5(3)	2.307(5)	0.0036(6)		
		Cl	2.5(2)	2.376(4)	0.0100(9)		
		C	3.6(7)	3.231(11)	0.0087(20)		
Zn,Al−BDC/Mo	Mo K	O	2.1(1)	1.712(2)	0.0049(3)	−2.2(5)	24.5
		Mo	2.0(5)	3.287(6)	0.0189(12)		

[a] CN = coordination number. Values in parentheses are statistical errors generated in EXCURVE. The true errors in coordination numbers are likely to be of the order of 20%; those for the interatomic distances are ca. 1.5%.[27] [b] Debye−Waller factor; σ = root-mean-square internuclear separation. [c] E_f = edge position (Fermi energy), relative to calculated vacuum zero. [d] $R = (\int[\Sigma^{\text{theory}} - \Sigma^{\text{exptl}}]k^3\,dk/[\Sigma^{\text{exptl}}]k^3\,dk) \times 100\%$. [e] Multiple scattering included for the linear unit Zn···ZA1···ZA2···Al with up to two different scattering atoms in any scattering path and a maximum total path length of 20 Å. [f] ZA1 = 0.47(2) Zn/0.53 Al; ZA2 = 0.50(13) Zn/0.50 Al. [g] ZA1 = 0.49(3) Zn/0.51 Al; ZA2 = 0.49(14) Zn/0.51 Al. [h] ZA1 = 0.50(4) Zn/0.50 Al; ZA2 = 0.50(23) Zn/0.50 Al. [i] Crystallographic bond distances:[32] Mo−O = 1.696, 1.695 Å; Mo−N = 2.310, 2.304 Å; Mo−Cl = 2.375, 2.370 Å.

cation distance), respectively, from the absorbing atom.[26] Details of the distribution are shown in Figure 3, which displays the portion of a cationic ordered sheet for a hypothetical LDH with $M^{II}/M^{III} = 2$. The theoretical curve shown in Figure 2 is for a seven-shell model (Table 1). Each shell was statistically significant, as measured by the reduced χ^2 test. The first shell comprises 5.5 oxygen atoms at 2.08 Å, consistent with zinc in octahedral coordination. According to the model shown in Figure 3, each divalent metal atom is surrounded by three M^{II} and three M^{III} at a and 6 M^{II} at $\sqrt{3}a$. To arrive at a bulk M^{II}/M^{III} ratio of 1.5, 10% of the divalent metal atoms in this model would have to be replaced by trivalent metal atoms. This means that, at the very least, the cation avoidance rule can no longer be sustained and there will be adjacent trivalent metal atoms. If we assume that the substitutions occur as far apart from each other as possible, then the predicted coordination numbers for the shell at a are 2.67 Zn and 3.33 Al. The Zn K-edge EXAFS of Zn,Al−NO_3 could be fitted by either 2.1 Zn at 3.08 Å or 2.1 Al at 2.99 Å (single scattering contributions only). However, neither fit was entirely satisfactory, and due to the proximity of the two shells, the structural parameters were highly correlated and it was not possible to include both shells in the same model. In the end, a significant improvement on either fit (by the reduced χ^2 test) was achieved by modeling the shell as a mixed site, i.e. Zn and Al backscatterers at the same distance (designated as ZA1). With the occupancy number fixed at 1, the composition of the site was optimized by including the fractional amount of Zn (F_{Zn}) in the refinement routine. A Zn:Al ratio of 0.47:0.53 was obtained for the seven-shell model with a coordination number of 6 and distance of 3.06 Å, i.e. 2.8 Zn and 3.2 Al. The refined value of F_{Zn} is quite close to the minimum theoretical value of 0.44 calculated for an LDH with $M^{II}/M^{III} = 1.5$. However, caution must be attached to the accuracy of F_{Zn} since the parameter is highly correlated with the interatomic distance $r_{Zn\cdots ZA1}$ and Debye−Waller factor $2\sigma^2_{Zn\cdots ZA1}$.[28]

The metal−metal distance of 3.059 Å is in excellent agreement with the value of a determined by X-ray diffraction. Using the EXAFS-derived distances for the first two shells, oxygen shells are expected at 3.70 Å (CN = 6, peak P3) and 4.80 Å (CN = 12, peak P4), and a Zn/Al shell is expected at 5.30 Å (CN = 6, peak P5). If one starts from

(26) Roussel, H.; Briois, V.; Elkaim, E.; de Roy, A.; Besse, J. P. *J. Phys. Chem. B* **2000**, *104*, 5915.

(27) Evans, J.; Gauntlett, J. T.; Mosselmans, J. F. W. *Faraday Discuss. Chem. Soc.* **1990**, 107.

(28) These relationships were examined in more detail by generating contour plots to show the variation of the fit index with either F_{Zn} and $r_{Zn\cdots ZA1}$ or F_{Zn} and $2\sigma^2_{Zn\cdots ZA1}$. For a 10% variation in the fit index, $F_{Zn} = 0.47 \pm 0.04$. The true error in F_{Zn} is likely to be of the order of 20%, similar to that usually associated with EXAFS-derived coordination numbers.

Scheme 1

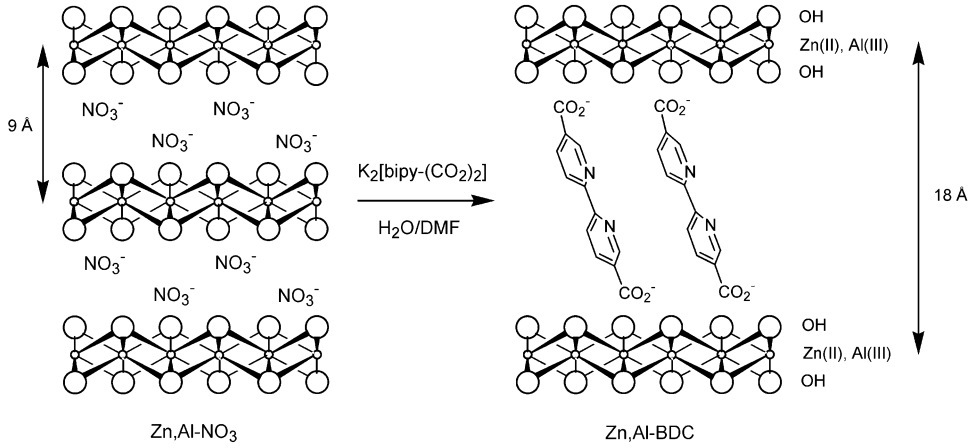

the two-shell model (single scattering contributions only), a marked improvement in the fit was obtained by adding a shell for six oxygens at 3.55 Å. Although this distance is considerably shorter than expected, the shell was judged to be statistically significant and was therefore included in the final fit. A further improvement in the simulation was obtained by adding a shell for 12 oxygens at 4.77 Å. The coordination number was fixed during the refinement procedure as it was found that allowing it to vary did not improve the quality of the fit sufficiently, as measured by the reduced χ^2 test. Although the statistical errors for this shell are quite large, the distance is close to that expected, and therefore, the shell was included in the final fit. The addition of a fifth shell for 6 Zn atoms at 5.30 Å brought about another significant improvement in the fit. Clearly, the refined coordination number and distance for this shell are in excellent agreement with the expected values. This shell could not be simulated as Al instead of Zn, and when modeled as a mixed site, the fractional amount of Zn refined to 0.9. This change produced only a very small improvement in the fit, and in fact the value of reduced χ^2 increased owing to the addition of another parameter in the refinement (fractional amount of Zn). Therefore in the final fit the shell was modeled as 6 Zn atoms.

The sixth and seventh shells, labeled as P6 and P8 in Figures 2 and 3, have contributions from Zn and Al backscatterers, and several solutions were possible within the distance ranges of 5.95−6.25 and 9.05−9.3 Å. The best overall fit was obtained by using a mixed site approximation (Zn/Al, $F_{Zn} = 0.5$) for the shell corresponding to P6 and 6 Al atoms for the shell corresponding to P8. Multiple scattering contributions were included for the linear unit comprising these two shells and the shell of 6 Zn atoms at 3.06 Å. The refined metal−metal distances of 6.14 and 9.19 Å are in good agreement with the expected values of 2*a* and 3*a*, respectively. The FT contains another peak corresponding to metallic neighbors at $\sqrt{7}a$ (P7). A shell for Zn atoms could indeed be fitted at 8.09 Å, but there was no significant improvement in the quality of the fit (by the reduced χ^2 test) and therefore the shell was not included in the final model. In conclusion, the EXAFS results show that the average local coordination environment of Zn in Zn,Al−NO_3 conforms to the model for an ordered cationic sheet. This is despite the fact that the existence of long-range cation ordering is not supported by powder XRD. As noted by Bellotto et al., long-range order is only routinely observed by powder XRD for Li,Al and Mg,Ga LDHs.[23]

The nitrate anions in Zn,Al−NO_3 were easily exchanged by 2,2′-bipyridine-5,5′-dicarboxylate (BDC) anions, as evidenced by elemental analysis, vibrational spectroscopy, and powder XRD. For example, the Raman spectrum of Zn,Al−BDC contained no band at about 1050 cm^{-1} for the symmetric stretching mode ν_1 of nitrate anions. Strong bands were observed at 1613 and 1389 cm^{-1} in the IR spectrum, assigned to ν_{as}(OCO) and ν_s(OCO) of carboxylate groups, respectively. Interestingly, the band associated with ν_{OH} stretching was broader than that exhibited by Zn,Al−NO_3 and two components were no longer observed. This seems to add weight to the above-mentioned stick-lying model for the arrangement of interlamellar nitrate anions. Upon intercalation of BDC anions, the d_{003} reflection shifted to 18.0 Å and six equally spaced 00*l* reflections were observed up to 30° 2θ (Figure 1). The longest dimension of the BDC anion was calculated as 14.2 Å (including van der Waals radii for the oxygen atoms), using the crystal structure data reported for a cobalt coordination polymer containing this anion.[29] A basal spacing of at least 19 Å would therefore be expected if the anions were lying perpendicular to the host layers. The observed spacing is shorter by 1 Å, suggesting that the anions are tilted slightly (Scheme 1).

The ^{13}C CP MAS NMR spectrum of Zn,Al−BDC exhibited several resonances in the range 120−150 ppm, assigned to carbon atoms of the bipyridyl groups, and a single peak at 169.3 ppm assigned to the carboxylate carbons. The Zn K-edge k^3-weighted EXAFS spectrum of Zn,Al−BDC was very similar to that for the Zn,Al−NO_3 precursor, confirming that no significant disruption of the layer structure occurred during intercalative ion exchange of the dicarboxylate anion (Figure 2). Although the useful data range was 13 $Å^{-1}$ rather than 14.5 $Å^{-1}$, the spectrum could be simulated by the seven-shell model (Table 1). The refined structural parameters are very similar to those obtained for the fit to the spectrum of

(29) Min, D.; Yoon, S. S.; Lee, S. W. *Inorg. Chem. Commun.* **2002**, *5*, 143.

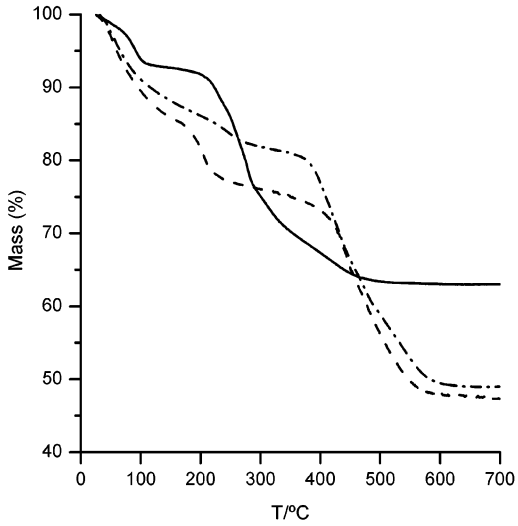

Figure 4. TGA curves of Zn,Al−NO_3 (—), Zn,Al−BDC (− − −), and Zn,Al−BDC/Mo (− · −).

Zn,Al−NO_3. The ^{27}Al MAS NMR spectra of Zn,Al−NO_3 and Zn,Al−BDC were also very similar (not shown). A sharp peak was observed at about 15.5 ppm with a broad low-frequency shoulder, assigned to octahedral aluminum. Similar spectra were obtained previously for Zn,Al LDHs pillared by ferrocenecarboxylate anions.[30] In that work the presence of two types of Al sites was confirmed by measuring triple-quantum ^{27}Al MAS NMR spectra. The first site, corresponding to the sharp peak, displays a distribution of isotropic chemical shifts and is probably due to the presence of a range of slightly different local Al environments generated by the random insertion of Al in the layers. The low-frequency shoulder is essentially undistributed, but it has an average quadrupole coupling constant[31] larger than the first site. We speculate that this site may be due to small clusters of Al atoms in the brucite-like layers.

Compounds Zn,Al−NO_3 and Zn,Al−BDC were also characterized by N_2 adsorption and thermogravimetric analysis. N_2 adsorption carried out on Zn,Al−NO_3 outgassed at room temperature overnight gave a BET specific surface area of less than 5 m^2 g^{-1}, indicating that the nitrogen molecules (kinetic diameter ca. 3.65 Å) cannot access the interlayer galleries. When nitrate anions were exchanged for BDC anions, an increase in nitrogen uptake was observed, most likely due to an increase in the interlayer void volume. The N_2 adsorption isotherm of Zn,Al−BDC (not shown) exhibits some adsorption at low relative pressures, followed by a sharp upward distortion at $p/p_0 > 0.7$. This may be due to capillary condensation inside the larger pores formed upon intercalation of the organic anions perpendicularly to the layers. These structural changes account for an increase in the BET specific surface area from less than 5 to 42 m^2 g^{-1}. Figure 4 shows the TGA curves for Zn,Al−NO_3 and Zn,-Al−BDC. The first weight loss for Zn,Al−NO_3 occurs from room temperature to 125 °C and is due to the removal of crystallization water (7%). A mass loss of 28.4% then takes place in the temperature range 200−500 °C, attributed to decomposition of the brucite-like layer and removal of interlayer anions. The water content in Zn,Al−BDC is higher as evidenced by a mass loss of 14.5% extending from room temperature to 160 °C. A second step is observed from 175 to 230 °C, assigned to partial dehydroxylation of the double hydroxide layers. Complete dehydroxylation of the lattice takes place from 390 to 590 °C, accompanied by elimination/decomposition of the organic anion.

Immobilization of Oxomolybdenum Complexes and Catalytic Studies. We anticipated that treatment of the Zn,-Al−BDC intercalate with a dichloromethane solution of the solvent adduct $MoO_2Cl_2(THF)_2$ (**1**) would result in the formation of a supported complex of the type MoO_2Cl_2(N−N). This was the method used to prepare the model compound MoO_2Cl_2(4,4′-dimethyl-2,2′-bipyridine) (**2**) and is in fact a general method for the synthesis of octahedral *cis*-MoO_2 complexes.[4] A slight excess of **1** was used, and elemental analysis of the final product, designated as Zn,-Al−BDC/Mo, gave 11.2 wt % Mo (1.17 mmol g^{-1}), indicating that nearly all metal complex in solution had been taken up. Accordingly, N_2 adsorption studies revealed a decrease in the BET specific surface area from 42 to 8 m^2 g^{-1}. The final material had a pale blue color, possibly due to the presence of some Mo^V centers. New bands were observed in the IR spectrum at 892 and 869 cm^{-1} assigned to Mo−O stretching vibrations (either Mo═O or Mo−O−Mo). The rest of the spectrum was largely unchanged compared with the spectrum for the Zn,Al−BDC precursor, showing in particular that no significant interaction had occurred between the carboxylate groups of BDC anions and the included molybdenum species. In accordance with these results, the ^{13}C CP MAS NMR spectrum of Zn,Al−BDC/Mo was very similar to that of Zn,Al−BDC except for peaks at 24.7 and 67.1 ppm attributed to THF molecules.

Mo K-edge EXAFS studies were carried out to probe the molecular structure of the molybdenum centers in Zn,Al−BDC/Mo. However, it must be remembered that where a structural diversity of metal species arises, the traditional approach to modeling the resultant EXAFS spectrum can give an indication only of the average structural environment.The room-temperature EXAFS of the model compound **2** was fitted by four shells corresponding to Mo−O_t, Mo−N_{bipy}, Mo−Cl, and Mo···C, in order of increasing distance from the absorbing atom (Figure 5, Table 1). The refined distances and coordination numbers are in good agreement with the known structure.[32] For the Mo K-edge EXAFS of Zn,Al−BDC/Mo, the presence of *cis*-MoO_2 units was confirmed by the fit of 2.1 oxygen atoms at 1.71 Å. However, no shells could be included for either Mo−Cl or Mo−N and instead the analysis revealed a shell for two molybdenum atoms at 3.29 Å. Decreasing the coordination number for this shell to one increased the value of reduced χ^2 by 4%. The average local coordination environment of Mo atoms in the material is therefore quite different from that in the

(30) Gago, S.; Pillinger, M.; Santos, T. M.; Rocha, J.; Gonçalves, I. S. *Eur. J. Inorg. Chem.* **2004**, 1389.
(31) Engelhardt, G.; Michel, D. *High-Resolution Solid-State NMR of Silicates and Zeolites*; Wiley: Chichester, U.K., 1987.
(32) Baird, D. M.; Yang, F. L.; Kavanaugh, D. J.; Finness, G.; Dunbar, K. R. *Polyhedron* **1996**, *15*, 2597.

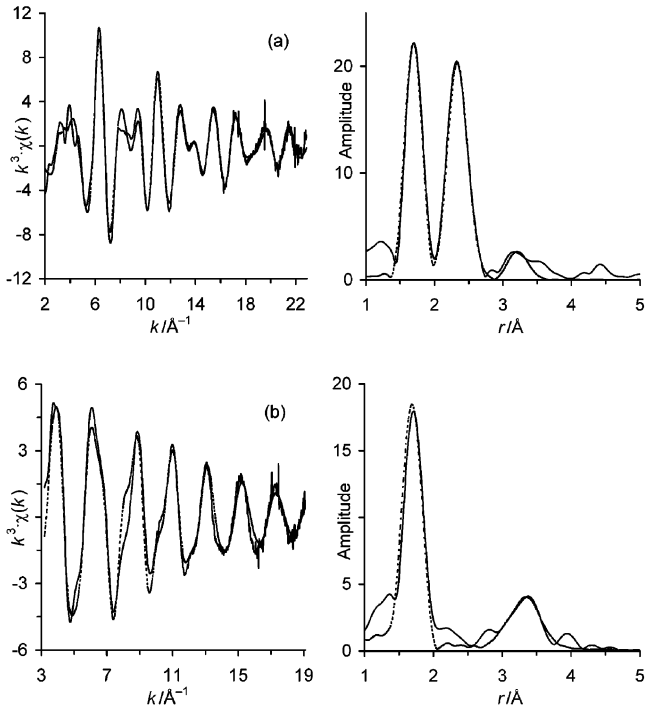

Figure 5. Room-temperature Mo K-edge EXAFS and Fourier transforms of (a) MoO_2Cl_2(4,4′-dimethyl-2,2′-bipyridine) (**2**) and (b) Zn,Al−BDC/Mo. The solid lines represent the experimental data, and the dashed lines show the best fits using the parameters given in Table 1.

model compound **2** (or the precursor **1**). The Mo−Cl bonds of **1** were broken during its encapsulation in the host LDH, culminating in the formation of oligomeric species, most likely unidentate-bridged species of the type Mo−O−Mo. The existence of such species was further supported by the fact that a slight improvement in the fit was obtained upon addition of a shell for oxygen atoms at 1.95 Å, corresponding to Mo−O bridging.[33] The statistical significance of this shell was questionable, and therefore, it was omitted from the final model. Nevertheless, the molybdenum species in Zn,Al−BDC/Mo are similar to those found previously for $MoO_2Cl_2(THF)_2$ immobilized in the mesoporous silica MCM-41 derivatized with bipyridyl groups (Mo···Mo = 3.28 Å).[9b] Oxybridged bimetallic species were also obtained after immobilization of $MoO_2(acac)_2$ in polymer supports carrying (((hydroxypropyl)amino)methyl)pyridine ligands.[6b,c]

Surprisingly, the Zn K-edge EXAFS spectrum of Zn,Al−BDC/Mo was quite different from that for Zn,Al−BDC (Figure 2). Although the frequency and fine structure of the oscillations are similar, there is an obvious decrease in amplitude for the molybdenum-containing material, especially toward high k values. In a comparison of the FTs, the intensity of P1 is approximately the same, while the peaks corresponding to the more distant metal−metal shells are considerably reduced for Zn,Al−BDC/Mo. This indicates that the brucite-like layers have been disrupted in some way, resulting in an increase in static disorder. In the fit to the EXAFS of Zn,Al−BDC/Mo, the oxygen shells at ca. 3.6 and 4.8 Å were no longer significant, and so a simplified five-shell model was used (Table 1). The best coordination number for the first shell was 5, while all other coordination numbers were fixed during the refinement procedure as it was found that allowing these to vary did not improve the quality of the fit sufficiently. Although the final fit is not very satisfactory, some conclusions can be drawn. The refined interatomic distances are not very different from those determined for Zn,Al−BDC. On the other hand, the Debye−Waller factors are higher, reflecting the apparent increase in static disorder. A possible explanation is that the complex $MoO_2Cl_2(THF)_2$ (**1**) reacted with the layer hydroxyl groups, resulting in covalent grafting of oxomolybdenum centers. This would be consistent with the Mo K-edge EXAFS results, which suggest that the chlorine neighbors were replaced by oxygen neighbors (although no evidence could be found for Mo···Zn/Al interactions). Complex **1** undergoes similar reactions with the surface silanol groups of ordered mesoporous silica.[34] A comparison of the TGA curves for Zn,Al−BDC and Zn,Al−BDC/Mo provides further support for the presence of an interaction between the host layers and the molybdenum guest species (Figure 4). The curves are similar except that the weight loss associated with partial dehydroxylation of the layers is considerably smaller for Zn,Al−BDC/Mo, indicating that the brucite-like layers were affected by the inclusion reaction. On the other hand, the ^{27}Al MAS NMR spectrum for the molybdenum-containing material was not different from that measured for the Zn,Al−BDC precursor.

The modified material Zn,Al−BDC/Mo was active as a catalyst for the liquid-phase epoxidation of *cis*-cyclooctene, 1-octene, and *trans*-2-octene using TBHP in anhydrous media at the reaction temperature of 55 °C, yielding the corresponding epoxides as the only products. A reaction carried out in the presence of Zn,Al−BDC and *cis*-cyclooctene gave less than 2% conversion after 8 h, confirming that the catalytically active sites in Zn,Al−BDC/Mo are predominantly oxomolybdenum species. The turnover frequency (TOF) for cyclooctene using Zn,Al−BDC/Mo was 6 mmol h^{-1} g^{-1} (calculated after 2 h). For comparison, a mesoporous silica functionalized with $MoO(O_2)_2$(L−L) complexes gave a TOF of 32 mmol h^{-1} g^{-1} for cyclooctene epoxidation using TBHP (carried out at 61 °C).[8] Concerning the different olefins used in the presence of Zn,Al−BDC/Mo, the reaction rates followed the order 1-octene (turnover number = 1.1 mmol g^{-1}; TOF = 0.1 mmol h^{-1} g^{-1}) < *trans*-2-octene (9.9; 1.4) < *cis*-cyclooctene (24.6; 3.5) (TON and TOF calculated after 7 h), in line with increasing substitution of the double bond by electron-donating alkyl groups. These results are consistent with a heterolytic mechanism involving an electrophilic oxidant. For complexes of the type $MoO_2Cl_2(L_1)(L_2)$ used in homogeneous catalytic olefin epoxidation, TBHP coordinates to the metal center, which acts as a Lewis acid increasing the electrophilicity of the peroxo moiety.[35] Cyclooctene epoxidation in homogeneous phase using the model complex MoO_2Cl_2(4,4′-dimethyl-2,2′-bipyridine) (**2**) was

(33) Third oxygen shell: Mo−O = 1.953(14) Å; $2\sigma^2$ = 0.0323(58) Å^2; CN = 1.0(5), R = 21.6%. The structural parameters for the other two shells were largely unchanged compared to those for the two-shell model given in Table 1.

(34) Nunes, C. D.; Valente, A. A.; Pillinger, M.; Rocha, J.; Gonçalves, I. S. *Chem.—Eur. J.* **2003**, *9*, 4380.

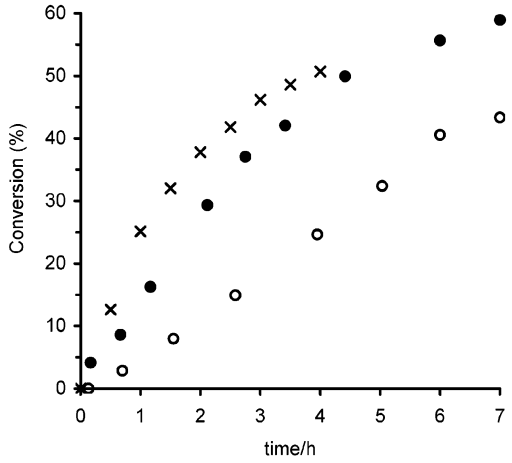

Figure 6. Cyclooctene epoxidation in the presence of Zn,Al−BDC/Mo [1st run (●), 2nd run (○)] and the homogeneous catalyst MoO_2Cl_2(4,4′-dimethyl-2,2′-bipyridine) (**2**) (×).

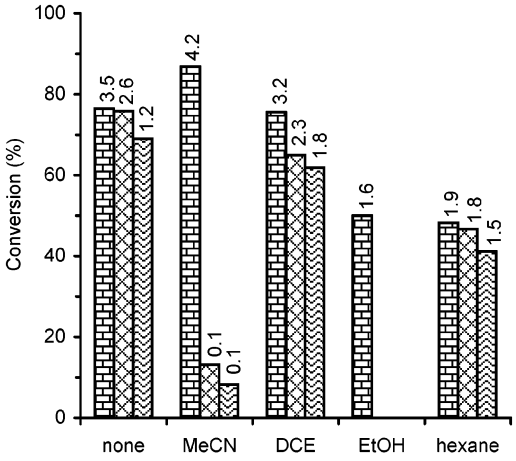

Figure 7. Cyclooctene conversion achieved after 24 h in the presence of Zn,Al−BDC/Mo [1st run (bricks), 2nd run (diamonds), 3rd run (waves)]. The turnover frequencies calculated after 7 h are indicated on top of the bars.

faster during the first 4 h than in the presence of Zn,Al−BDC/Mo (initial reaction rates of 25 and 5 mol mol_{Mo}^{-1} h^{-1}, respectively, under similar reaction conditions). An agitation speed of ca. 700 rpm was used to avoid external mass transfer limitations. However, internal diffusion limitations in the case of Zn,Al−BDC/Mo might affect the reaction rate. On the other hand, differences in the coordination spheres of the molybdenum centers in the free and supported metal complexes may account for the different catalytic activities. The kinetic profiles of cyclooctene epoxidation using Zn,Al−BDC/Mo or complex **2** are similar, suggesting that the reaction takes place through a similar mechanism (Figure 6). The conversion increases steadily up to about 5 h, but then the reaction starts to slow, reaching 76% conversion after 24 h. This retardation effect has previously been attributed to the competitive coordination of *tert*-butyl alcohol, a byproduct of TBHP, to the molybdenum centers. With aqueous TBHP the epoxidation of *cis*-cyclooctene in the presence of Zn,Al−BDC/Mo was much slower (15% conversion after 24 h). A possible explanation is that water is a strongly coordinating solvent which may lead to the formation of less stable molybdenum complexes. On the other hand, the adsorption of polar water molecules inside the hydrophilic inorganic host may have adverse effects on the reaction rate by creating internal diffusion limitations.

The influence of the solvent, namely hexane, 1,2-dichloroethane (DCE), ethanol (EtOH), or acetonitrile (MeCN), on the catalytic performance was studied using TBHP at 55 °C. Selectivity toward cyclooctene oxide was always 100%. The reaction rate increased in the order EtOH < hexane < DCE < no additional solvent < MeCN (Figure 7). No direct relationship between solvent polarity and catalytic activity could be established. As mentioned above, coordinating solvents may retard the reaction by competing for coordination sites. For example, the reaction is slower with EtOH than with DCE. However, this does not satisfactorily explain the observed results since MeCN gives the highest reaction rate. Another possible explanation is the influence of the solvent on the catalyst stability toward leaching of the active metal species into the liquid phase. Hence, the catalyst stability was studied for each solvent by recycling the catalyst twice. The solid was separated from the reagents and products by centrifuging, washed with dichloromethane, and dried at room-temperature overnight prior to reuse. When the solvent was DCE or *n*-hexane or when no solvent was added, cyclooctene conversion after 24 h decreased by less than 14% in three cycles (Figure 7). In the case of MeCN or EtOH, nearly complete or even complete loss of catalytic activity was observed after the first run. A possible explanation is the favorable adsorption of the more polar solvents on the hydrophilic inorganic support, which may lead to solvolysis of the oxomolybdenum centers and subsequent loss of catalytic activity in the following runs. The molybdenum loading of the recovered solids was determined by ICP-AES. Approximately 16% Mo was released from the LDH when the solvent was MeCN, whereas for DCE or without solvent no metal leaching was detected. Evidence of real heterogeneous catalysis using Zn,Al−BDC/Mo and either no additional solvent or DCE was obtained by carrying out duplicate reactions in which the solid was separated at the reaction temperature after 2 h and the solution was stirred for another 5 h. For both solvents substrate conversion in solution increased less than 5% compared to ca. 30% observed in the presence of a catalyst.

Concluding Remarks

A layered double hydroxide pillared by 2,2′-bipyridine-5,5′-dicarboxylate has successfully been prepared by ion exchange and examined as a "solid ligand" for the immobilization of oxomolybdenum complexes. The material exhibits a high encapsulating ability, but the presence of a supported complex of the type MoO_2Cl_2(bipy) could not be proven. Instead, the EXAFS results indicate that the major species are oxo-bridged oligomers, which may be covalently linked to the brucite-like layers. The molybdenum-containing material is an active and recyclable catalyst for the selective

(35) Kühn, F. E.; Groarke, M.; Bencze, É.; Herdtweck, E.; Prazeres, A.; Santos, A. M.; Calhorda, M. J.; Romão, C. C.; Gonçalves, I. S.; Lopes, A. D.; Pillinger, M. *Chem.—Eur. J.* **2002**, *8*, 2370.

epoxidation of olefins. The stability is superior to that reported for a material prepared by immobilization of $MoO_2Cl_2(THF)_2$ in the mesoporous silica MCM-41 derivatized with bipyridyl groups.[9b] Questions remain about the actual nature of the catalytically active centers. As proposed for certain polymer-supported oxomolybdenum complexes,[6b] the Mo−O−Mo bonds in Zn,Al−BDC/Mo could be ruptured upon reaction with TBHP, yielding active mononuclear Mo^{VI} centers coordinated by *t*-$BuOO^-$ groups. Mo K-edge EXAFS studies of a recovered catalyst may help to shed light on this problem. In the future we will also be examining the ability of the Zn,Al−BDC intercalate to chelate other transition metal ions from solution, e.g. Co^{2+}, Ni^{2+}, and Cu^{2+}.

Acknowledgment. This work was partly funded by the FCT, POCTI, and FEDER (Project POCTI/QUI/37990/2001). S.G. thanks the University of Aveiro for a research grant. We also acknowledge the European Synchrotron Radiation Facility for provision of synchrotron radiation facilities and thank Olivier Mathon for assistance in using beamline BM29.

IC049755N